ORGANIC CHEMISTRY FRONTIERS

RESEARCH ARTICLE

View Article Online
View Journal



Cite this: DOI: 10.1039/d6qo00377j

# Enantioselective synthesis of tetrahydrofurans by permanganate-mediated oxidative cyclisation of 1,5-dienes using chiral phase-transfer catalysis

Nikita S. Rank, [a] Aqeel A. Hussein, [a,b] Alexander L. Cecil,[a] Mark E. Light[a] and Richard C. D. Brown *[a]

Permanganate-mediated oxidative cyclisation of 1,5-dienes under chiral phase transfer catalysis (CPTC) conditions provides 2,5-dihydroxyalkyl substituted tetrahydrofurans (THF-diols) wherein four new C–O bonds are established with excellent control of relative and absolute stereochemistry. Structurally complex THF-containing motifs found in a host of bioactive natural products are accessible by oxidative transformation of simple dienes, which is exemplified by formal syntheses of *cis*-solamin A. Electron-withdrawing ester or ketone groups in the substrates – conjugated to one alkene of the 1,5-diene system – direct the initial manganation reaction to the electron-deficient alkene, which proceeds with enantiofacial selectivity in the presence of the CPTC. Cinchona alkaloid scaffolds are a convenient platform for chiral quaternary ammoniums with short synthetic routes to anthracenylmethyl and 3,5-bis(trifluoromethyl-benzyl) CPTC derivatives realising enantioselectivities up to 89–94% ee for structurally distinct 1,5-diene systems using a readily-available and inexpensive oxidant. DFT calculations provide significant new mechanistic insight into the permanganate-mediated reaction supporting the involvement of a protonated Mn(v) glycolate in THF ring-formation through enhanced electrophilicity of the metal oxo intermediate. Furthermore, calculations identify the interplay between dipole-driven electrostatic stabilisation and cooperative noncovalent interactions in the transition state complex for manganation in the first reaction step, leading to the observed facial selectivity in this powerful synthetic reaction.

Received 25th March 2026,
Accepted 10th May 2026

DOI: 10.1039/d6qo00377j

rsc.li/frontiers-organic



## Introduction

Tetrahydrofurans (THFs) are key structural features of numerous bioactive compounds, with prominent examples including polyether ionophore antibiotics and Annonaceous acetogenins.[1] The THF ring systems in these natural products are often substituted with stereo-defined hydroxyalkyl groups at their 2- and 5-positions, rendering such "THF-diol" motifs enduring targets for asymmetric synthesis.[1f,2] Oxidative cyclisation using transition-metal-oxo species such as $MnO_4^-$,[3] $OsO_4$,[4] and $RuO_4$,[5] is exceptional in providing direct access to THF-diols **2** from 1,5-dienes **1** with the creation of four new C–O bonds, and up to four new stereocentres in a single reaction (Scheme 1(a)).[6] Access to enantiomerically enriched THF-diols **4a** has been realised by permanganate-mediated oxidative cyclisation of dienoyl systems **3a** bearing chiral auxiliaries (Scheme 1(b)).[7] To date, analogous asymmetric processes using Ru- or Os oxo species have proved elusive, although oxidative cyclisation of enantiomerically-enriched hex-5-ene-1,2-diols **6** has been accomplished using these catalysts and Cr oxo reagents (Scheme 1(c)).[6d,8]

We discovered that asymmetric oxidative cyclisation of 2,6-dienones **3b** was possible in the presence of a chiral phase-transfer catalyst (CPTC) **5a** giving enantioenriched THF diols **4b** (Scheme 1(b)),[9] demonstrating the concept of achieving stereoinduction through chiral ion pairing with permanganate. Subsequently, asymmetric permanganate-promoted dihydroxylation,[10] and oxohydroxylation[10a,11] have been developed under CPTC. Most recently, an asymmetric oxidative cyclisation of 1,4-dienes has been reported using quaternary ammonium CPTC.[12]

Despite the novelty of our original CPTC 1,5-diene oxidative cyclisation, enantioselectivities of up to 75% ee were moderate and the use of aryl-2,6-dienones **3b** as substrates restricted flexibility for onwards transformation of the THF products **4b**. Accordingly, the potential of this asymmetric process to access valuable THF diol fragments warranted further investigation, particularly given the ability to deliver structural complexity with control over relative and absolute stereochemistry using

[a]*School of Chemistry and Chemical Engineering, University of Southampton, Southampton, Hampshire, SO17 1BJ, UK. E-mail: R.C.Brown@soton.ac.uk*
[b]*Department of Biology, College of Science, Al-Qasim Green University, 51013 Al-Qasim, Babylon, Iraq*

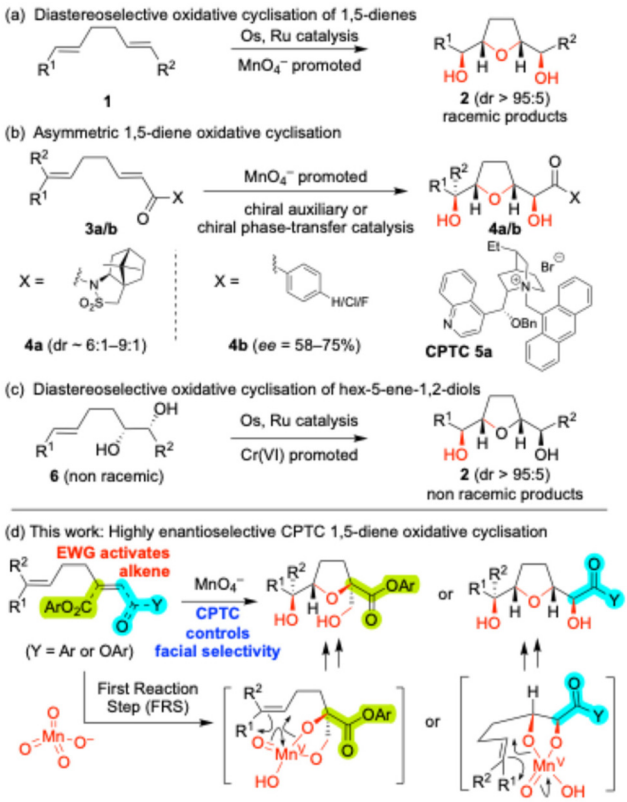


**Scheme 1** Oxidative cyclisation of 1,5-dienes and enediols using metal oxo species.

an inexpensive oxidising agent, benign metal byproducts and easily accessible catalyst. In the present work, we show that oxidative cyclisation of 1- and 2-carboxyaryl-1,5-hexadienes (dienoates) and 1-aroyl-1,5-hexadienes (dienones) of different structural types can be realised under CPTC conditions to afford THF diols with high levels of enantiocontrol (Scheme 1(d)). The utility of the process is illustrated through formal syntheses of the bioactive acetogenin *cis*-solamin A from two different oxidative cyclisation products, each obtained with >90% ee. DFT calculations are presented to gain understanding of the role of acid in the cyclisation step and the interactions giving rise to the observed enantioinduction in the anionic CPTC-manganation transition state (TS) complexes.

## Results and discussion

### Optimisation and substrate scope

Asymmetric induction in the THF diol products arising from 1,5-diene oxidative cyclisation is determined during the first reaction step (FRS), namely manganation of the more reactive alkene (Scheme 1d). α,β-Unsaturated ketones and carboxylic acid derivatives are good initiators of permanganate cyclisations due to the activating effect of electron-withdrawing groups on alkene reactivity.[7,9,12–14] In the present optimisation an enoate ester functioned as the initiator group, wherein aryl groups delivered promising levels of asymmetric induction. Aryl esters also facilitate onwards transformations of the resulting THF diols towards bioactive natural products. On this basis the 2-naphthyl dienoate **7a** was selected for optimisation using *N*-anthracenylmethyl cinchonidinium **5a** as CPTC (Table 1).[9,15] The racemic THF diol ***rac*-8a** was obtained from **7a** in 70% yield using Adogen 464 in acetone/AcOH.[16]

The preferred solid-liquid CPTC conditions – finely ground $KMnO_4$ (1.6 equiv.), catalyst **5a** (10 mol%) and AcOH (6.5 equiv.) in $CH_2Cl_2$ at −60 to −50 °C – afforded the enantioenriched THF diol **8a** in 70% yield and 71% ee (entry 1, Table 1). $KMnO_4$ is insoluble in $CH_2Cl_2$ and without the CPTC a low yield (15%) of the racemic THF diol **8a** was obtained, also recovering unreacted diene (80%, entry 2). The small amount of conversion seen in the absence of CPTC was attributed to solubilisation of $MnO_4^-$ taking place during the aqueous work-up.

Increasing the amount of CPTC to 30 mol% offered a modest increase in ee to 75% (entry 3), and a lower loading of 5 mol% led to a small erosion of enantioselectivity (68% ee, entry 4). Temperatures above −50 °C also gave diminished enantioselectivities (entries 5 and 6). Omitting AcOH resulted in incomplete conversion of starting material with formation of the alkenediol **9a** in 10% yield with comparable enantioselectivity (ee = 70%, entry 7) to that obtained for the THF diol **8a**. The preference for dihydroxylation products from permanganate oxidation of alkenes under neutral or basic conditions is well-established.[10,17] This experiment also confirmed preference for initial reaction of permanganate ion at the elec-

**Table 1** Influence of reaction conditions on yield and enantioselectivity for CPTC oxidative cyclisation of dienoate **7a**[a]

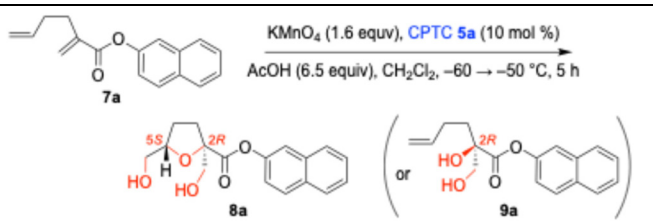


| Entry | Deviation from standard conditions | Yield[a] (%) 8a | 9a | ee[b] (%) |
|---|---|---|---|---|
| 1 | None | 70 | —[c] | 71 |
| 2 | CPTC **5a** (0 mol%) | 15[d] | —[c] | 0 |
| 3 | CPTC **5a** (30 mol%) | 60 | —[c] | 75 |
| 4 | CPTC **5a** (5 mol%) | 64 | — | 68 |
| 5 | −20 → −30 °C | 52 | —[c] | 59 |
| 6 | 0 °C | 67 | —[c] | 49 |
| 7 | AcOH (0 equiv.) | —[e] | 10 | 70 |

Reactions conducted on 0.20 mmol scale. [a] Isolated yields. [b] ee determined by chiral HPLC analysis. [c] Diol **9a** not observed when AcOH was present. [d] Starting diene **7a** recovered (80%). [e] Starting diene **7a** recovered (20%).

tron-poor enoate alkene and that acidic conditions are necessary for cyclisation of the intermediate Mn glycolate.

With promising enantioselectivity (>70% ee) achieved for a dienoate substrate using CPTC **5a**, attention turned to the influence of the chiral quaternary ammonium structure (Table 2).[18] Five additional readily accessible dihydrocinchonidinium CPTCs **5b–e**, **10d** and pseudo-enantiomeric dihydrocinchonium **11d** were applied to the oxidative cyclisation of 2-naphthyl ester **7a** (Table 2). Pleasingly, all benzyl ether derivatives **5a–e** returned THF diols with moderate to high ee values (entries 1–5), with the highest selectivity (89% ee) and yield (78%) realised using the 3,5-bis(trifluoromethylbenzyl) ammonium salt **5d** (entry 4). The other fluorinated derivative – 2,3,4-trifluorobenzylammonium **5e** – provided the second highest enantioselectivity (81% ee, entry 5) among the cinchonidinium catalysts investigated. The carbinol catalyst **10d** performed very poorly both in terms of rates of conversion of **7a** and enantioselectivity compared to its benzyl ether **5d** (entry 6, Table 2). This finding is consistent with previous proposals that ether substituents may serve as a blocking group in these CPTCs, which – in combination with the N-$CH_2$Ar group – control ion pairing in the TS complex.[19]

Application of the pseudo-enantiomeric catalyst **11d** – obtained in three steps from cinchonine – afforded the enantiomeric THF diol ***ent*-8a** with improved 91% ee highlighting the flexibility of the CPTC approach (entry 7, Table 2). The absolute stereochemistry of THF diol ***ent*-8a** was determined as (2*S*,5*R*) using single crystal X-ray diffraction (Fig. 1).[20] On this basis, and corroborated by X-ray structural assignment for **13b** below,[20] the major enantiomers **8a–k** were assigned (2*R*,5*S*).

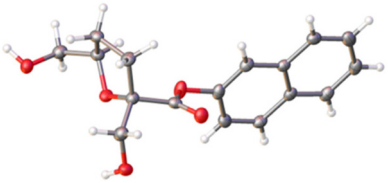

**Fig. 1** Absolute stereochemistry of ***ent*-8a** (2*S*,5*R*) determined using single crystal X-ray diffraction. Thermal ellipsoids shown at 50% probability.

At this juncture, the influence of the aryl ester group on enantioselectivity was investigated for substrates **7b–k** (Table 3). Reactions were carried out under the conditions

**Table 2** Influence of CPTC structure on enantioselectivity for oxidation of dienoate **7a**

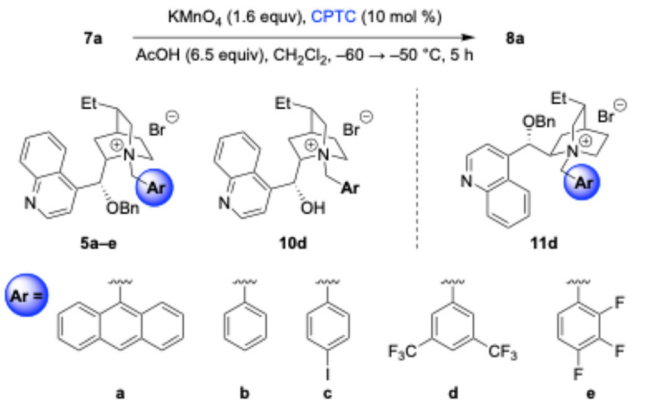


| Entry | CPTC | Yield of **8a**[a] (%) | ee (%) |
|---|---|---|---|
| 1 | **5a** | 70 | 71 |
| 2 | **5b** | 37 | 74 |
| 3 | **5c** | 70 | 70 |
| 4 | **5d** | **78** | **89** |
| 5 | **5e** | 6[b] | 81 |
| 6 | **10d** | 22[c] | 10 |
| 7 | **11d** | 41 (***ent*-8a**) | 91[d] |

[a] Isolated yields. [b] Unreacted starting material **7a** (54%) recovered. [c] Unreacted starting material **7a** (40%) recovered. [d] ***ent*-8a** (2*S*,5*R*) is the major enantiomer obtained.

**Table 3** Enantioselective oxidative cyclisation of aryl dienoates **7**

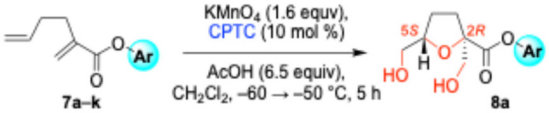


| | | Yield **8a–k**[a] (%) [ee[b] (%)] | | |
|---|---|---|---|---|
| Entry | Ar | Using PTC[c] | Using CPTC **5a** | Using CPTC **5d** |
| 1 | **a** | 53 [*rac*] | 60 [75] | **78 [89]** ***ent*-8a**, 41 [91][d] |
| 2 | **b** | 58 [*rac*] | 71 [65] | 73 [68] ***ent*-8b**, 78 [78][d] |
| 3 | **c** | 52 [*rac*] | 58 [45] | 56 [74] |
| 4 | **d** | 55 [*rac*] | — | 41 [76][e] |
| 5 | **e** | 56 [*rac*] | 40 [71][e] | 18 [70][e] |
| 6 | **f** | 36 [*rac*] | 55 [59][e] | **76 [89]** |
| 7 | **g** | 88 [*rac*] | 84 [52] | 81 [82] |
| 8 | **h** | 70 [*rac*] | 32 [61] | 38 [79][e] |
| 9 | **i** | 74 [*rac*] | — | 33 [57] |
| 10 | **j** | 70 [*rac*] | — | 16 [57][e] |
| 11 | **k** | 94 [*rac*] | 73 [62] | 58 [72] |

[a] Isolated yields. [b] Determined using chiral HPLC. [c] Adogen 464 (10 mol%), $KMnO_4$ (1.3 equiv.), acetone/AcOH (3 : 2), −30 to −10 °C, 3 h. [d] Reactions using pseudo-enantiomeric CPTC **11d** gave ***ent*-8a** (entry 1) and ***ent*-8b** (entry 2). [e] Starting material recovered: **7d** (15%); **7e** (34%) using CPTC **5a**, (25%) using CPTC **5d**; **7f** (20%); **7h** (34%); **7j** (72%).

optimised for **7a** using two CPTCs, **5a** and **5d**. In some cases the reactions did not reach completion in 5 h and the starting dienes were recovered (see table footnotes).[21] With respect to enantioselectivity, the new CPTC **5d** out-performed the original *N*-anthracenylmethyl ammonium **5a** for all but one ester substrate where a similar ee value was obtained (entry 5). Aryl esters with *ortho*-substituents gave enantioselectivities in the range 70–89% ee (entries 4–8) using CPTC **5d**. The highest selectivity was observed for the 2-methoxyphenyl ester **7f** (89% ee, 76% yield, entry 6) matching that for the 2-naphthyl ester **7a** (89% ee, 78% yield, entry 1). Interestingly, the 1-naphthyl ester **7b** gave a significantly lower enantioselectivity (68% ee, entry 2) using CPTC **5d** compared to its regioisomer **7a** (89% ee, entry 1). A notable improvement in the magnitude of the ee for the THF diol ***ent*-8b** (78% ee, entry 2) was obtained using the pseudo-enantiomeric CPTC **11d**.

Dienoates **12** containing a pendant trisubstituted alkene were investigated using the optimised conditions (Table 4).[21] The best performing substrates again proved to be the 2-naphthyl and 2-methoxyphenyl esters **12a** and **12f**, affording THF diols **13a** and **13f** in good yields and 84% ee using catalyst **5d**. A modest reduction in selectivity – compared to monosubstituted alkenes – may be due to the interaction of the alkenyl group with the catalyst, but some conversion with low selectivity initiated at the trisubstituted alkene cannot be excluded. A crystal structure for the major enantiomer **13b** was obtained (see SI),[20] affirming the absolute stereochemical assignments for the series.

2-Naphthyl hepta-2,6-dienoate **14** is a representative model substrate towards polyether and acetogenin natural products (Scheme 2). Pleasingly, oxidative cyclisation of **14** using CPTC **5d** afforded the THF diol **15** with 92% ee and 40% yield, demonstrating the potential to achieve highly enantioselectivity in a different substrate type. A lower ee of 75% was obtained using the original (9-anthacenyl)methylammonium

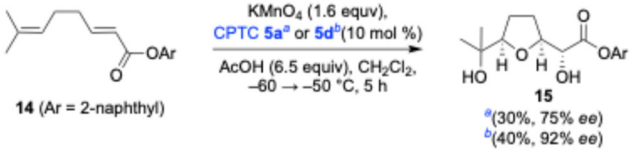


**Scheme 2** CPTC oxidative cyclisation of hepta-2,6-dienoate **14**.

catalyst **5a**. These results highlight the ability to optimise selectivity within different diene structural types through simple manipulations of a common readily available CPTC scaffold.

Our original report disclosed the oxidative cyclisation of a relatively small subset of aryl 2,6-dienone substrates under CPTC conditions to give THF diols with ee values 58–75%.[9] Further investigation of aryl dienones – varying the aryl groups in **16a–c** and **18a–d** – revealed that highly enantioselective transformations are possible in the presence of CPTC **5a** (Tables 5 and 6). Indeed, several THF diol products were obtained with ee values exceeding 90% (Table 5, entry 1 and Table 6, entries 3 and 4). The 1-naphthyl substrate **16a** provided excellent selectivity (93% ee, Table 5, entry 1). Phenyl ketone **16b** gave the corresponding THF diol **17b** with a modest 54% ee (entry 2), while an *ortho* substituent in **16c** increased selectivity (entry 3).

Extending the polyaromatic system in the 9-anthracenyl ketone **18a** apparently shut down oxidative cyclisation under CPTC conditions, giving a complex mixture of oxidation products (Table 6, entry 1). Oxidation under achiral conditions afforded the racemic THF diol ***rac*-19a** in only 5% yield, indicating that steric hindrance of the 9-anthryl group – twisted out of the plane of the carbonyl – impeded initial permanganate addition.

Racemic oxidation of the 2-methoxy substituted 1-naphthyl ketone **18b** afforded THF diol ***rac*-19b** in 76% yield (entry 2). Under CPTC conditions, however, the yield was substantially reduced to 43% and the enantioselectivity was completely eroded (entry 2; *cf.* Table 5, entry 1). On the other hand,

**Table 4** Enantioselective oxidative cyclisation of aryl dienoates **12**

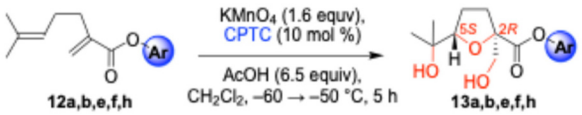


| | | Yield **13a,b,e,f** and **h**[a] (%) [ee[b] (%)] | | |
|---|---|---|---|---|
| Entry | Ar | Using PTC[c] | Using CPTC **5a** | Using CPTC **5d** |
| 1 | **a** 2-Naphthyl | 70 [*rac*] | — | 68 [**84**][d] |
| 2 | **b** 1-Naphthyl | 51 [*rac*] | 76 [61][e] | 88 [71] |
| 3 | **e**  | 73 [*rac*] | 60 [69] | 40 [70][e] |
| 4 | **f** 2-$MeOC_6H_4$ | 59 [*rac*] | — | 75 [**84**] |
| 5 | **h** 2-$ClC_6H_4$ | 76 [*rac*] | — | 68 [81] |

[a] Isolated yields. [b] Determined using chiral HPLC. [c] Adogen 464 (10 mol%), $KMnO_4$ (1.3 equiv.), acetone/AcOH (3 : 2), −30 to −10 °C, 3 h. [d] Primary alcohol acetylated prior to chiral HPLC analysis. [e] Starting material recovered **12b** (4%); **12e** (20%).

**Table 5** Enantioselective oxidative cyclisation of aryl 2,6-dienones **16a–c**

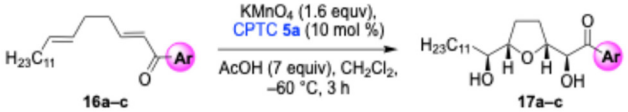


| | | Yield **19a–e**[a] (%) [ee][b] (%) | |
|---|---|---|---|
| Entry | Ar | Using PTC[c] | Using CPTC **5a** |
| 1 | **a** 1-Naphthyl | 46 [*rac*] | **42 [93]** |
| 2 | **b** Ph | 50 [*rac*] | 43 [54] |
| 3 | **c** 2-Tolyl | 35 [*rac*] | 34 [71] |

[a] Isolated yields. [b] Determined using chiral HPLC. [c] Adogen 464 (10 mol%), $KMnO_4$ (1.3 equiv.), AcOH (16 equiv.), acetone, −30 to −10 °C, 1.5 h.

**Table 6** Enantioselective oxidative cyclisation of aryl 2,6-dienones **18a–d**

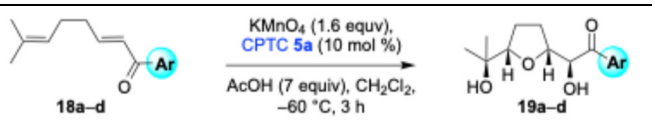


| Entry | Ar | Yield **19a–d**[a] (%) [ee[b] (%)] Using PTC | Using CPTC **5a** |
|---|---|---|---|
| 1 | **a** | 5 [*rac*][c,d] | 0[d] |
| 2 | **b** | 76 [*rac*][e] | 43 [<5] |
| 3 | **c** | 81 [*rac*][e] | 43 **[92]** |
| 4 | **d** | 66 [*rac*][e] | 42 **[94]**, 55 [90][f] 40 [39][g] |

[a] Isolated yields. [b] Determined using chiral HPLC. [c] Adogen 464 (10 mol%), $KMnO_4$ (1.3 equiv.), AcOH (16 equiv.), acetone, −30 to −10 °C, 1.5 h. [d] A complex mixture of products was obtained. [e] Adogen 464 (10 mol%), $KMnO_4$ (1.3 equiv.), acetone/AcOH (3 : 2), −30 to −10 °C, 1 h. [f] Reaction conducted at −60 to −50 °C, 6 h. [g] Using CPTC **5d**.

4-fluoro-1-naphthyl ketone and the 2,3-dichlorophenyl ketone both gave very high levels of asymmetric induction (92 and 94% ee) with the CPTC catalyst **5a** (Table 6, entries 3 and 4). The 3,5-bis(trifluoromethylbenzyl)ammonium CPTC **5d** was not effective for enantioselective ketone oxidation, affording the THF diol **18d** with a greatly diminished 39% ee (entry 4).

The absolute stereochemistry of the major enantiomeric 4-fluoro-1-naphthyl ketone **19c** was established by X-ray diffraction after derivatisation as its mono 3-bromobenzoyl ester **20** (Fig. 2).[20,22] An intriguing observation is that the absolute configuration within the THF diol moiety is reversed for the ketone series compared to the corresponding aryl ester systems (*cf.* THF diol **15**, Scheme 2). The factors contributing to facial selectivity are discussed below.

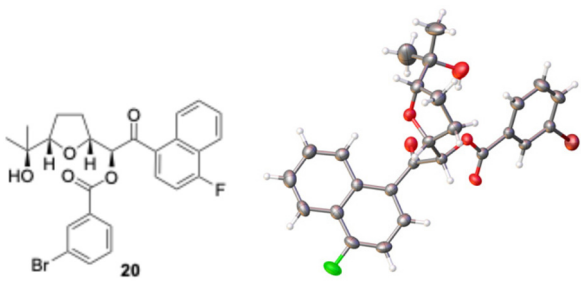


**Fig. 2** Absolute stereochemistry of 3-bromobenzoate derivative **20** determined using single crystal X-ray diffraction. Thermal ellipsoids are shown at 50% probability.

## Formal synthesis of *cis*-solamin A (26)

The value of enantiomerically enriched aryl ketone and aryl ester oxidative cyclisation products obtained from CPTC oxidative cyclisation was highlighted through application to formal syntheses of *cis*-solamin A (**26**, Schemes 3 and 4).[23,24] Asymmetric cyclisation of dienone **21** using CPTC catalyst **5a** at −40 °C gave the THF diol **22** in 52% yield and 92% ee on a 0.5 g scale (Scheme 3).[25] Initial attempts to effect regioselective Baeyer–Villiger oxidation of diol **22** or its diacetate **23** proved fruitless, leading to oxidative cleavage of the side-chain to afford a lactone. Therefore, a three-step oxidative cleavage of the arene system was implemented. Thus, borohydride reduction of ketone **23** afforded a mixture of epimeric carbinols, which underwent Ru-catalysed oxidative cleavage and reaction with *O*-methyl-*N*,*N*′-diisopropylisourea to afford the methyl ester **24**.[26,27] Finally, reduction of ester **24** using $LiAlH_4$ secured the enantiomerically enriched triol **25**, which is an intermediate previously used in total syntheses of *cis*-solamin A.[8d,23d,e,24]

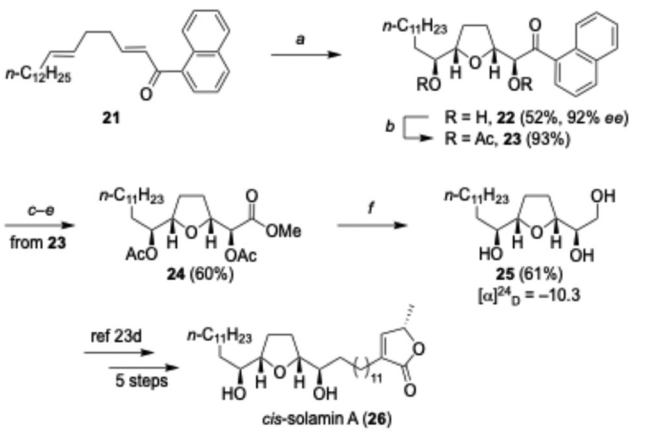


**Scheme 3** Formal synthesis of *cis*-solamin A (**26**) from aryl dienone **21**. Reagents and conditions: (a) $KMnO_4$ (1.6 equiv.), CPTC **5a** (10 mol%), AcOH (8 equiv.), $CH_2Cl_2$, −40 °C, 3 h.; (b) AcCl (5 equiv.), pyr (10 equiv.), DMAP (2.5 equiv.), $CH_2Cl_2$, 0 °C, 1.5 h; (c) $NaBH_4$ (1.2 equiv.), MeOH, −10 °C, 25 min; (d) $RuCl_3{\cdot}H_2O$ (20 mol%), $H_5IO_6$ (15 equiv.), $CH_3CN$, $CCl_4$, $H_2O$, 3 h; (e) *O*-methyl-*N*,*N*′-diisopropylisourea (1.6 equiv.), THF, reflux, 4 h; (f) $LiAlH_4$ (5 equiv.), $Et_2O$, 0 °C, 30 min.

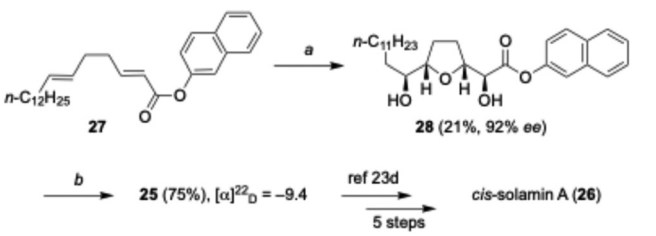


**Scheme 4** Formal synthesis of *cis*-solamin A (**26**) from dienoate **27**. Reagents and conditions: (a) $KMnO_4$ (1.6 equiv.), CPTC **11d** (10 mol%), AcOH (6.5 equiv.), $CH_2Cl_2$, −60 °C, 5 h.; (b) $NaBH_4$ (2.0 equiv.), $THF/H_2O$ (3 : 1), −20 to −10 °C, 3 h.

An analogous aryl 2,6-dienoate **27** was also oxidised under CPTC conditions using pseudo-enantiomeric CPTC **11d** (Scheme 4), securing THF diol **28** in 21% yield (92% ee). Diene **27** (12%) and an uncyclized α,β-diketoester byproduct (<5%) were also isolated.[28] From ester **28** conversion to the *cis*-solamin A triol **25** was trivial, using borohydride reduction. Comparison of the specific rotation values of the triol **25** samples obtained from dienone and dienoate oxidative cyclisation products **22** and **28** with literature values confirmed their absolute stereochemistry to be the same. This corroborated the reversal of facial selectivity exhibited by the enone and enoate systems, giving rise to the same enantiomeric triols by using pseudo-enantiomers of the CPTC.

## Mechanism and stereochemistry

Permanganate oxidative cyclisation is highly diastereoselective for the 2,5-*cis*-disubstituted THF stereoisomer, with stereospecific vicinal dioxygenation of each alkene by the metal oxo species.[29] Based upon the original proposal of Baldwin *et al.* a plausible step-wise mechanism is shown for a simple dienoate ester **29** (Fig. 3a).[29a] The first reaction step involves [3 + 2] cycloaddition of permanganate ion and diene **29** to form the Mn(v) glycolate intermediate **30**. As discussed above, the presence of the conjugated electron-withdrawing carbonyl group directs the addition of permanganate to the enoate alkene in the first reaction step. The rate acceleration is consistent with stabilisation of an electron-rich transition state **TS1** by the conjugated carbonyl group.[13] Thus, developing negative charge in the first reaction step TS manifests in an increased interaction between the carbonyl oxygen of the substrate and the chiral quaternary ammonium giving rise to asymmetric induction.[9] Prior to addressing the factors contributing to enantiofacial selectivity in this first reaction step, computational analysis of the cyclisation using density functional theory (DFT) calculations is provided.

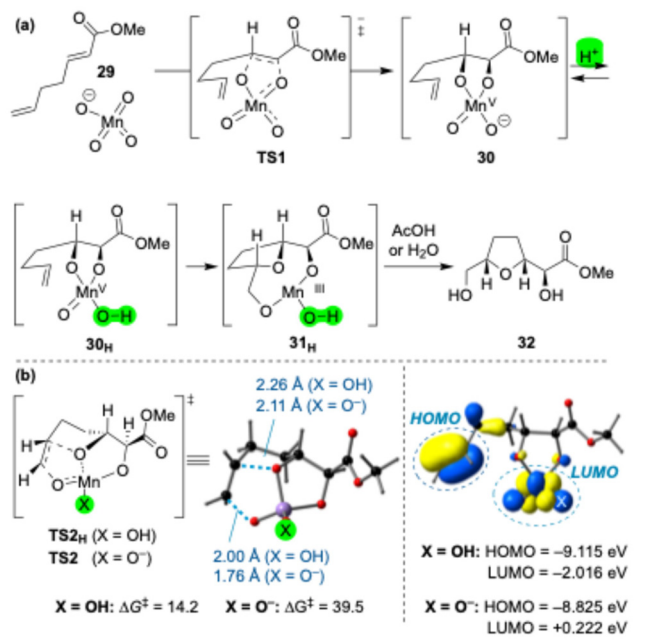


**Fig. 3** (a) Proposed mechanism for the oxidative cyclisation of methyl (*E*)-hepta-2,6-dienoate (**29**) by $MnO_4^-$ in the presence of AcOH. (b) Transition states for anionic and protonated THF ring formation. Free energies are in kcal $mol^{-1}$.

Although it is reported that reoxidation of the Mn(v) centre in glycolate **30** to Mn(vi) is required for the THF ring-formation to proceed,[29a] DFT calculation find comproportionation of **30** with permanganate to be highly unfavourable.[30,31] Furthermore, it is clear from experimental studies that manganate ion (Mn(vi)) actually disproportionates rapidly under acidic conditions, giving hypomanganate (Mn(v)) and permanganate (Mn(vii)).[32] Therefore, it is reasonable to conclude that the THF-forming step should proceed through an Mn(v) intermediate under the oxidative cyclisation reaction conditions.

A previous computational study concluded that an intermediate Mn(v) glycolate is able to cyclise onto the pendant alkene leading to the THF diol after hydrolysis.[30] However, mildly acidic conditions – $CO_2$ ebullition or AcOH – are necessary to obtain cyclised products, and in absence of acid vicinal dihydroxylation is the major pathway (see Table 1, entry 7).[10c] Therefore, it is plausible that the Mn(v) glycolate **30** undergoes protonation under acid conditions, increasing the electrophilicity of the metal oxo species $\mathbf{30_H}$ to promote reaction with the second alkene *via* $\mathbf{TS2_H}$.[13] Indeed, our DFT calculations lend support to this hypothesis, observing a substantially lower barrier of 14.4 kcal $mol^{-1}$ for cyclisation of the protonated glycolate $\mathbf{30_H \rightarrow 31_H}$ compared to 39.5 kcal $mol^{-1}$ for the anionic pathway *via* **TS2** (Fig. 3b). Enhanced electrophilicity of the protonated Mn(v) intermediate $\mathbf{30_H}$ is evident from LUMO localisation at the Mn site.

To shed light onto the interactions leading to enantioselectivity, DFT calculations were performed including the CPTC in the first reaction step.[33,34] We sought to reconcile the high and opposing facial selectivity outcomes observed for the ester and ketone substrates (Fig. 4). The 2-naphthyl ester **7a** and model 1-naphthyl ketone (**33**, right) systems were selected for investigation using the cinchonidinium CPTCs **5d** and **5a**, respectively, as these catalysts provide the highest levels of enantioinduction for the respective substrates.[35] Considering the 2-naphthyl ester **7a** first, TSs arising from reaction at its *Re* and *Si* faces involve asynchronous (3 + 2) cycloaddition of $MnO_4^-$ with more advanced development of the $C_\beta$–O bond compared to the $C_\alpha$–O bond (Fig. 5a). The $\mathbf{TS_{(2R)}}$ – consistent with the major enantiomeric product **8a** derived from *Si* face approach – is calculated to be lower in energy than $\mathbf{TS_{(2S)}}$ by 1.52 kcal $mol^{-1}$. For the aryl ketone substrate model calculations find the $\mathbf{TS_{(1'S,2R)}}$ to be 2.5 kcal $mol^{-1}$ lower in energy compared to the $\mathbf{TS_{(1'R,2S)}}$ (Fig. 5b). Again, this result is consistent with the observed major product, which is formed from approach of the oxidant from below the plane of the enone as depicted in Fig. 4 and 5.

To better understand the computational results we performed distortion/interaction analysis (DIA)[36] and calculated

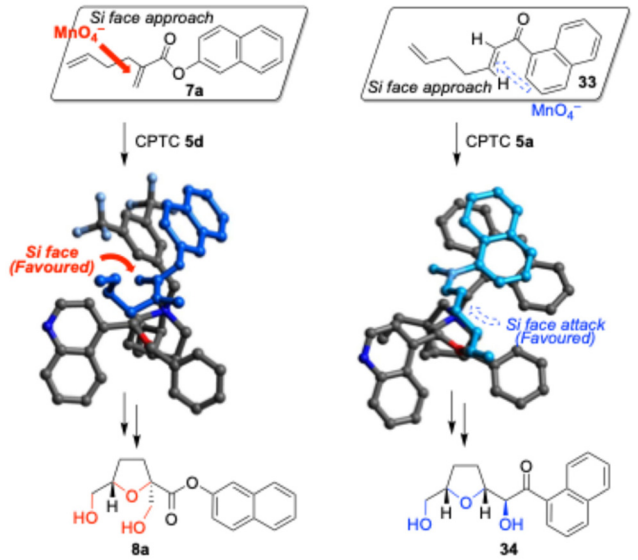


Fig. 4 Observed facial selectivity outcomes from permanganate oxidation of ester and ketone substrates using cinchonidinium CPTCs **5a** and **5d**.

intermolecular noncovalent interactions (NCIs) using the independent gradient model based on the Hirschfeld (IGMH) partition of the molecular density (Fig. 5c).[37,38] The DIA calculations for the ester $\mathbf{TS_{(2R)}}$ show a greater stabilisation energy ($\Delta E_{int}$ = −3.0 *vs.* −0.73 kcal mol$^{-1}$) and lower total distortion energy (11.05 *vs.* 13.01 kcal mol$^{-1}$) compared to $\mathbf{TS_{(2S)}}$, leading to reduce the overall barrier (8.05 *vs.* 12.28 kcal mol$^{-1}$). According to NCI analysis, $\mathbf{TS_{(2R)}}$ features strong π–π stacking interactions and cation–π interactions between the naphthyl group of the ester and the $CH_2$ groups adjacent to the quaternary nitrogen and bis(trifluoromethyl)phenyl (BTFMP) group of CPTC **5d**. Crucially, nonclassical C–H···O hydrogen bonding between the ester carbonyl oxygen and the same $CH_2$ groups contributes towards stabilisation. Electrostatic stabilisation of this interaction is enhanced due to charge separation between $MnO_4^-$ and the positively charged ammonium and a larger dipole moment ($\mu$ = 17.1 D) with greater electron density at the carbonyl oxygen. The $\mathbf{TS_{(2S)}}$ leading to the minor enantiomer maintains strong π–π stacking between the substrate naphthyl and the BTFMP group of the CPTC. However, it lacks the stabilising hydrogen bond between the ester carbonyl and the ammonium $CH_2$ groups, and instead $MnO_4^-$ remains localized near the positively charged region as indicated from the

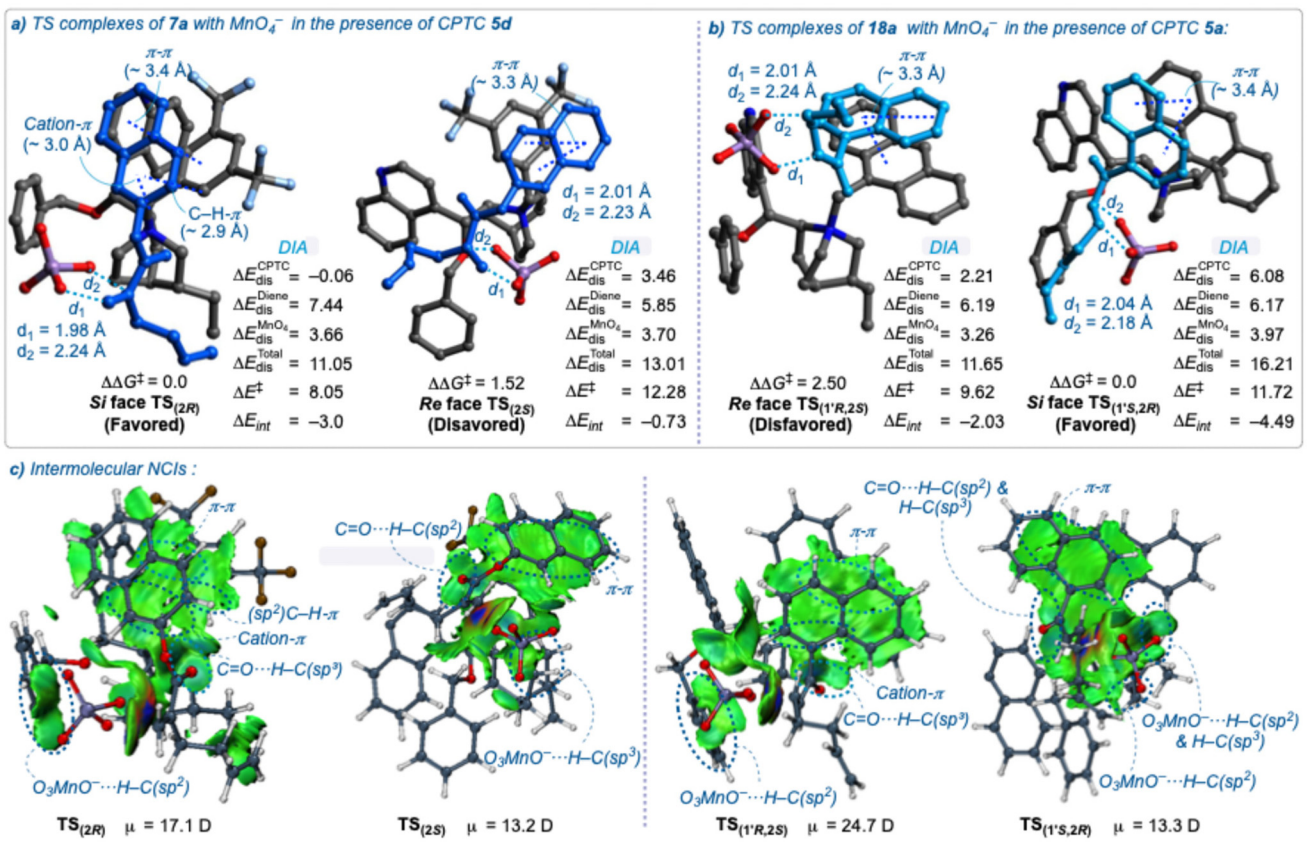


Fig. 5 DFT computed transition states for the enantioinduction step involving (3 + 2) cycloaddition of $MnO_4^-$ and the electron-deficient alkene for (a) 2-naphthyl dienoate **7a** in presence of CPTC **5d** and (b) 1-naphthyl 2,6-dienone **33** in presence of CPTC **5a** computed at 213.15 K. (c) Intermolecular NCIs calculated using the IGMH method. Energies are in kcal mol$^{-1}$.

reduced dipole ($\mu$ = 13.2 D), contributing to its relatively higher energy.

For dienone oxidations of the 1-naphthyl ketone, $\mathbf{TS_{(1'S,2R)}}$ is more stable than $\mathbf{TS_{(1'R,2S)}}$ by 2.5 kcal mol$^{-1}$, consistent with the observed enantiofacial selectivity. Although $\mathbf{TS_{(1'S,2R)}}$ exhibits higher distortion (16.21 *vs.* 11.65 kcal mol$^{-1}$) and intrinsic activation energies (11.72 *vs.* 9.62 kcal mol$^{-1}$), it benefits from more than twice the stabilisation energy of $\mathbf{TS_{(1'R,2S)}}$ (−4.49 *vs.* −2.03 kcal mol$^{-1}$). NCI analysis identifies cooperative interactions in $\mathbf{TS_{(1'S,2R)}}$, including naphthyl-anthryl π-π stacking and multiple non-classical H-bonding between Mn–O and C═O oxygens of the bound TS with C(sp$^2$)–H and C(sp$^3$)–H groups of the ammonium catalyst. These interactions stabilise $\mathbf{TS_{(1'S,2R)}}$ while keeping its dipole nearly unchanged (13.3 D *vs.* 12.8 D) from the pre-TS complex. The $\mathbf{TS_{(1'R,2S)}}$ also features π–π and cation–π interactions, but the carbonyl primarily engages with $CH_2$ groups of the ammonium, raising the dipole (24.7 D *vs.* 18.0 D in the pre-TS complex) and reducing net stabilisation. Overall, the stereochemical outcome originates from favourable stabilisation of $\mathbf{TS_{(1'S,2R)}}$ due to a balance of moderate dipole and cooperative noncovalent interactions.

## Conclusions

Highly enantioselective oxidative cyclisation of 1,5-dienes to give THF diols has been realised using easily accessible chiral phase-transfer catalysts and inexpensive oxidant. The quaternary ammonium catalyst structure can be readily modified to achieve high levels of enantioinduction (89–94% ee) across different diene types containing initiator enone or enoate groups. Furthermore, the synthetic ultility towards bioactive compounds is highlighted by formal syntheses of the Annonaceous acetogenin natural product *cis*-solamin A (**26**). Enantiocontrol is established during the first reaction step due to selective ion pairing between the chiral quaternary ammonium and the anionic manganation TS. DFT calculations identify the interplay between dipole-driven electrostatic stabilisation and cooperative noncovalent interactions in the TS complex, giving rise to the observed facial selectivity. Furthermore, calculations support the proposal that the THF-forming reaction step proceeds through a protonated Mn(v) glycolate intermediate $\mathbf{30_H}$, extending our mechanistic understanding of this powerful synthetic method.

## Author contributions

Nikita Rank: investigation (lead); writing – original draft preparation. Aqeel Hussein: investigation; methodology (computational lead); writing – original draft. Alexander Cecil: investigation. Mark Light: investigation (crystallography). Richard Brown: conceptualisation; supervision; writing – review and editing.

## Conflicts of interest

There are no conflicts to declare.

## Data availability

The data supporting this article have been included as part of the supplementary information (SI). Supplementary information: NMR spectra, experimental details, crystallographic data, and computational details. See DOI: **https://doi.org/10.1039/d6qo00377j**.

CCDC 2334832 (***ent*-8a**), 2372158 (**13b**), 2476423 (**20**) and 2354449 (**11d**) contain the supplementary crystallographic data for this paper.[20a–d]

## Acknowledgements

The authors acknowledge financial support from Savita Rank, Suresh Rank, and Ankita Rank (studentship NR), the office of the Iraqi Prime Minister (HCED/Iraq, studentship AAH) and The Royal Society (University Research Fellowship to RCDB). N. Wells (NMR) and J. Herniman (MS) supported collection of characterisation data through the respective NMR (EP/K039466/1 and EP/W006480/1) and MS (EP/K039466/1 and EP/S033343/1) Facilities. Calculations were performed using the IRIDIS High Performance Computing Facility, and associated support services at the University of Southampton, and the DICC High Performance Computing Facility at Universiti Malaya with support from Prof. A. Ariffin (Universiti Malaya).

## References

1 For selected reviews of bioactive natural products containing tetrahydrofurans. Annonaceous Acetogenins. (*a*) A. Bermejo, B. Figadère, M. C. Zafra-Polo, I. Barrachina, E. Estornell and D. Cortes, Acetogenins from Annonaceae: recent progress in isolation, synthesis and mechanisms of action, *Nat. Prod. Rep.*, 2005, **22**, 269–303; (*b*) N. G. Li, Z. H. Shi, Y. P. Tang, J. W. Chen and X. A. Li, Progress in Total Synthesis of Annonaceous Acetogenins from Annonaceae, *Chin. J. Org. Chem.*, 2009, **29**, 350–364; (*c*) C. C. Liaw, J. R. Liou, T. Y. Wu, F. R. Chang and Y. C. Wu, Acetogenins from Annonaceae, *Prog. Chem. Org. Nat. Prod.*, 2016, **101**, 113–230; (*d*) R. Tundis, J. B. Xiao and M. R. Loizzo, Annona species (Annonaceae): a rich source of potential antitumor agents?, *Ann. N. Y. Acad. Sci.*, 2017, **1398**, 30–36; (*e*) A. Neske, J. R. Hidalgo, N. Cabedo and D. Cortes, Acetogenins from Annonaceae family. Their potential biological applications, *Phytochemistry*, 2020, **174**, 112332; (*f*) M. M. Faul and B. E. Huff, Strategy and Methodology Development for the Total Synthesis of Polyether Ionophore Antibiotics, *Chem. Rev.*, 2000, **100**, 2407–2473; (*g*) M. Antoszczak, J. Rutkowski and A. Huczynski, Structure and Biological Activity of Polyether

 

Ionophores and Their Semisynthetic Derivatives, *Bioactive Nat. Prod. Chem. Biol.*, 2015, 107–170; (*h*) A. Huczynski, Polyether Ionophores – Promising Bioactive Molecules for Cancer Therapy, *Bioorg. Med. Chem. Lett.*, 2012, **22**, 7002–7010; (*i*) H. Liu, S. Q. Lin, K. M. Jacobsen and T. B. Poulsen, Chemical Syntheses and Chemical Biology of Carboxyl Polyether Ionophores: Recent Highlights, *Angew. Chem., Int. Ed.*, 2019, **58**, 13630–13642; THF-containing macrolides.(*j*) A. Lorente, J. Lamariano-Merketegi, F. Albericio and M. Alvarez, Tetrahydrofuran-Containing Macrolides: A Fascinating Gift from the Deep Sea, *Chem. Rev.*, 2013, **113**, 4567–4610.

2 For selected reviews (*a*) Z. Zhong and X.-S. Peng, 3.07 - Furans and Their Benzo Derivatives: Synthesis, in *Comprehensive Heterocyclic Chemistry IV*, ed. D. S. Black, J. Cossy and C. V. Stevens, Elsevier, Oxford, 2022, pp. 307–411, DOI: 10.1016/B978-0-12-409547-2.14769-9; (*b*) Q. L. Lu, D. S. Harmalkar, Y. Choi and K. Lee, Discovery of Indoleamine 2,3-Dioxygenase 1 (IDO-1) Inhibitors Based on Ortho-Naphthaquinone-Containing Natural Product, *Molecules*, 2019, **24**, 3778; (*c*) A. de la Torre, C. Cuyamendous, V. Bultel-Poncé, T. Durand, J. M. Galano and C. Oger, Recent advances in the synthesis of tetrahydrofurans and applications in total synthesis, *Tetrahedron*, 2016, **72**, 5003–5025; (*d*) J. D. Rainier, Synthesis of Substituted Tetrahydrofurans, *Top. Heterocycl. Chem.*, 2014, **35**, 1–41; (*e*) G. Jalce, X. Franck and B. Figadère, Diastereoselective synthesis of 2,5-disubstituted tetrahydrofurans, *Tetrahedron Asymmetry*, 2009, **20**, 2537–2581; (*f*) J. P. Wolfe and M. B. Hay, Recent advances in the stereoselective synthesis of tetrahydrofurans, *Tetrahedron*, 2007, **63**, 261–290.

3 E. Klein and W. Rojahn, Die permanganatoxydation von 1,5-dienverbindungen, *Tetrahedron*, 1965, **21**, 2353–2358.

4 (*a*) M. de Champdoré, M. Lasalvia and V. Piccialli, OsO4-Catalyzed oxidative cyclization of geranyl and neryl acetate to cis-2,5-bis(hydroxymethyl)tetrahydrofurans, *Tetrahedron Lett.*, 1998, **39**, 9781–9784; (*b*) T. J. Donohoe and S. Butterworth, A General Oxidative Cyclization of 1,5-Dienes Using Catalytic Osmium Tetroxide, *Angew. Chem., Int. Ed.*, 2003, **42**, 948–951.

5 (*a*) S. Roth, S. Göhler, H. Cheng and C. B. W. Stark, A Highly Efficient Procedure for Ruthenium Tetroxide Catalyzed Oxidative Cyclizations of 1,5-Dienes, *Eur. J. Org. Chem.*, 2005, 4109–4118; (*b*) V. Piccialli and N. Cavallo, *Tetrahedron Lett.*, 2001, **42**, 4695–4699; (*c*) L. Albarella, D. Musumeci and D. Sica, Reactions of 1,5-Dienes with Ruthenium Tetraoxide: Stereoselective Synthesis of Tetrahydrofurandiols, *Eur. J. Org. Chem.*, 2001, 997–1003; (*d*) P. H. J. Carlsen, T. Katsuki, V. S. Martin and K. B. Sharpless, A greatly improved procedure for ruthenium tetroxide catalyzed oxidations of organic compounds, *J. Org. Chem.*, 1981, **46**, 3936–3938.

6 For selected reviews.(*a*) J. Adrian, L. J. Gross and C. B. W. Stark, The direct oxidative diene cyclization and related reactions in natural product synthesis, *Beilstein J. Org. Chem.*, 2016, **12**, 2104–2123; (*b*) V. Piccialli, *Molecules*, 2014, **19**, 6534–6582; (*c*) N. S. Sheikh, Comparative perspective and synthetic applications of transition metal mediated oxidative cyclisation of 1,5-dienes towards cis-2,5-disubstituted tetrahydrofurans, *Org. Biomol. Chem.*, 2014, **12**, 9492–9504; (*d*) B. S. Pilgrim and T. J. Donohoe, Osmium-Catalyzed Oxidative Cyclization of Dienes and Their Derivatives, *J. Org. Chem.*, 2013, **78**, 2149–2167; (*e*) V. Piccialli, Oxidative Cyclization of Dienes and Polyenes Mediated by Transition-Metal-Oxo Species, *Synthesis*, 2007, 2585–2607, DOI: 10.1055/s-2007-983835.

7 (*a*) A. M. Al Hazmi, N. S. Sheikh, C. J. R. Bataille, A. A. M. Al-Hadedi, S. V. Watkin, T. J. Luker, N. P. Camp and R. C. D. Brown, trans-2-Tritylcyclohexanol as a Chiral Auxiliary in Permanganate-Mediated Oxidative Cyclization of 2-Methylenehept-5-enoates: Application to the Synthesis of trans-(+)-Linalool Oxide, *Org. Lett.*, 2014, **16**, 5104–5107; (*b*) R. C. D. Brown and P. J. Kocienski, A Synthesis of Salinomycin. Part 1. Synthesis of Key Fragments, *Synlett*, 1994, 415–417; (*c*) C. L. Morris, Y. L. Hu, G. D. Head, L. J. Brown, W. G. Whittingham and R. C. D. Brown, Oxidative Cyclization Reactions of Trienes and Dienynes: Total Synthesis of Membrarollin, *J. Org. Chem.*, 2009, **74**, 981–988; (*d*) N. S. Sheikh, C. J. Bataille, T. J. Luker and R. C. D. Brown, Enantioselective Formal Synthesis of Eurylene: Synthesis of the cis- and trans-THF Fragments Using Oxidative Cyclization, *Org. Lett.*, 2010, **12**, 2468–2471; (*e*) D. M. Walba, C. A. Przybyla and C. B. Walker, Total synthesis of ionophores. 6. Asymmetric induction in the permanganate-promoted oxidative cyclization of 1,5-dienes, *J. Am. Chem. Soc.*, 1990, **112**, 5624–5625.

8 For examples of *cis*-selective oxidative cyclisations of dihydroxyalkenes. Mediated by Cr(VI).(*a*) E. J. Corey and D. C. Ha, Total synthesis of venustatriol, *Tetrahedron Lett.*, 1988, **29**, 3171–3174; (*b*) B. D. Hammock, S. S. Gill and J. E. Casida, Synthesis and morphogenetic activity of derivatives and analogs of aryl geranyl ether juvenoids, *J. Agric. Food Chem.*, 1974, **22**, 379–385; (*c*) D. M. Walba and G. S. Stoudt, Oxidative cyclization of 5,6-dihydroxyalkenes promoted by Cr(VI) oxo species: A novel cis-2,5-disubstituted tetrahydrofuran synthesis, *Tetrahedron Lett.*, 1982, **23**, 727–730Catalysed by Os(VI)/(VIII) see ref. 6*d* and. (*d*) T. J. Donohoe and S. Butterworth, Oxidative Cyclization of Diols Derived from 1,5-Dienes: Formation of Enantiopure cis-Tetrahydrofurans by Using Catalytic Osmium Tetroxide; Formal Synthesis of (+)-cis-Solamin, *Angew. Chem., Int. Ed.*, 2005, **44**, 4766–4768; (*e*) T. J. Donohoe, K. M. R. Wheelhouse, P. J. Lindsay-Scott, P. A. Glossop, I. A. Nash and J. S. Parker, Pyridine-N-Oxide as a Mild Reoxidant Which Transforms Osmium-Catalyzed Oxidative Cyclization, *Angew. Chem., Int. Ed.*, 2008, **47**, 2872–2875; Catalysed by Ru.(*f*) H. Cheng and C. B. W. Stark, A Double Donor-Activated Ruthenium(VII) Catalyst: Synthesis of Enantiomerically Pure THF-Diols, *Angew. Chem., Int. Ed.*, 2010, **49**, 1587–1590.

9 R. C. D. Brown and J. F. Keily, Asymmetric Permanganate-Promoted Oxidative Cyclization of 1,5-Dienes by Using Chiral Phase-Transfer Catalysis, *Angew. Chem., Int. Ed.*, 2001, **40**, 4496–4498.

10 (*a*) P. L. Gu, S. S. Wang, X. X. Wen, J. X. Tian, C. Wang, L. L. Zong and C. H. Tan, Asymmetric permanganate dihydroxylation of enoates: substrate scope, mechanistic insights and application in bicalutamide synthesis, *Org. Chem. Front.*, 2024, **11**, 836–842; (*b*) C. Wang, L. L. Zong and C. H. Tan, Enantioselective Oxidation of Alkenes with Potassium Permanganate Catalyzed by Chiral Dicationic Bisguanidinium, *J. Am. Chem. Soc.*, 2015, **137**, 10677–10682; (*c*) R. A. Bhunnoo, Y. L. Hu, D. I. Lainé and R. C. D. Brown, An Asymmetric Phase-Transfer Dihydroxylation Reaction, *Angew. Chem., Int. Ed.*, 2002, **41**, 3479–3480.

11 (*a*) X. R. Chen, J. X. Tian, S. S. Wang, C. Wang and L. L. Zong, Toward Bicalutamide Analogues with High Structural Diversity Using Catalytic Asymmetric Oxohydroxylation, *J. Org. Chem.*, 2024, **89**, 3907–3911; (*b*) S. Q. Li, S. S. Wang, J. Li, Y. Qi, C. Wang, L. L. Zong and C. H. Tan, Monocationic Cinchoninium Catalyzed Asymmetric Oxohydroxylation of Enoates, *ACS Catal.*, 2021, **11**, 15141–15148.

12 During the preparation of this manuscript Wen *et al.* reported CPTC oxidative cyclisation of 1,4-diene systems, achieving high enantioselectivities; X. Wen, S. Wang, R. Li, S. Wang, F. Wang, W. Zhong, C. Wang and L. Zong, Asymmetric Permanganate Oxidative Cyclization of 1,4-Dienoates Enables Direct Access to Chiral Tetrahydrofurans, *Org. Lett.*, 2025, **31**, 8522–8528.

13 D. G. Lee and K. C. Brown, Oxidation of hydrocarbons. 11. Kinetics and mechanism of the reaction between methyl (E)-cinnamate and quaternary ammonium permanganates, *J. Am. Chem. Soc.*, 1982, **104**, 5076–5081.

14 R. C. D. Brown, C. J. Bataille, R. M. Hughes, A. Kenney and T. J. Luker, Permanganate Oxidation of 1,5,9-Trienes: Stereoselective Synthesis of Tetrahydrofuran-Containing Fragments, *J. Org. Chem.*, 2002, **67**, 8079–8085.

15 (*a*) E. J. Corey and F. Y. Zhang, Mechanism and Conditions for Highly Enantioselective Epoxidation of α,β-Enones Using Charge-Accelerated Catalysis by a Rigid Quaternary Ammonium Salt, *Org. Lett.*, 1999, **1**, 1287–1290; (*b*) B. Lygo and P. G. Wainwright, A new class of asymmetric phase-transfer catalysts derived from Cinchona alkaloids - Application in the enantioselective synthesis of α-amino acids, *Tetrahedron Lett.*, 1997, **38**, 8595–8598; (*c*) B. Lygo and P. G. Wainwright, Asymmetric phase-transfer mediated epoxidation of α,β-unsaturated ketones using catalysts derived from Cinchona alkaloids, *Tetrahedron Lett.*, 1998, **39**, 1599–1602.

16 For further details see SI.

17 S. Dash, S. Patel and B. K. Mishra, Oxidation by permanganate: synthetic and mechanistic aspects, *Tetrahedron*, 2009, **65**, 707–739.

18 For selected reviews chiral phase-transfer catalysis (*a*) T. Marcelli and H. Hiemstra, *Cinchona Alkaloids in Asymmetric Organocatalysis, Synthesis*, 2010, pp. 1229–1279, DOI: 10.1055/s-0029-1218699; (*b*) T. Ooi and K. Maruoka, Recent Advances in Asymmetric Phase-Transfer Catalysis, *Angew. Chem., Int. Ed.*, 2007, **46**, 4222–4266; (*c*) J. Vachon and J. Lacour, Recent Developments in Enantioselective Phase Transfer Catalysis Using Chiral Ammonium Salts, *Chimia*, 2006, **60**, 266–275; (*d*) X. Yang, Y. Deng, D. Ling, T. Li, L. Chen and Z. Jin, Recent Progress in Chiral Quaternary Ammonium Salt-Promoted Asymmetric Nucleophilic Additions, *ACS Catal.*, 2025, **15**, 1973–2001; (*e*) D. C. M. Albanese and M. Penso, New Trends in Asymmetric Phase Transfer Catalysis, *Eur. J. Org. Chem.*, 2023, e202300224; (*f*) D. Qian and J. Sun, Recent Progress in Asymmetric Ion-Pairing Catalysis with Ammonium Salts, *Chem. – Eur. J.*, 2019, **25**, 3740–3751; (*g*) H.-J. Lee and K. Maruoka, Asymmetric phase-transfer catalysis, *Nat. Rev. Chem.*, 2024, **8**, 851–869; (*h*) W. Wu, C. Liu, C.-H. Tan and X. Ye, The Role of Anions in Guanidinium-Catalyzed Chiral Cation Ion Pair Catalysis, *Acc. Chem. Res.*, 2025, **58**, 2269–2281; (*i*) L. L. Zong and C. H. Tan, Phase-Transfer and Ion-Pairing Catalysis of Pentanidiums and Bisguanidiniums, *Acc. Chem. Res.*, 2017, **50**, 842–856.

19 E. J. Corey, F. Xu and M. C. Noe, A Rational Approach to Catalytic Enantioselective Enolate Alkylation Using a Structurally Rigidified and Defined Chiral Quaternary Ammonium Salt under Phase Transfer Conditions, *J. Am. Chem. Soc.*, 1997, **119**, 12414–12415.

20 (*a*) CCDC 2334832: Experimental Crystal Structure Determination, for ***ent*-8a**, 2026, DOI: 10.5517/ccdc.csd.cc2jcl5p; (*b*) CCDC 2354449: Experimental Crystal Structure Determination, for **11d**, 2026, DOI: 10.5517/ccdc.csd.cc2k0zzk; (*c*) CCDC 2476423: Experimental Crystal Structure Determination, for **20**, 2026, DOI: 10.5517/ccdc.csd.cc2p3xmc; (*d*) CCDC 2372158: Experimental Crystal Structure Determination, for **13b**, 2026, DOI: 10.5517/ccdc.csd.cc2kmf7w.

21 Amounts of recovered starting dienes are reported in table footnotes. No attempt was made to increase conversion further for these examples.

22 The absolute stereochemistry of **20** is also consistent with that for the corresponding 4-bromoketone reported in our preliminary communication (see ref. 9).

23 For total syntheses of *cis*-solamins A and B.(*a*) H. Göksel and C. B. W. Stark, Total Synthesis of cis-Solamin: Exploiting the RuO4-Catalyzed Oxidative Cyclization of Dienes, *Org. Lett.*, 2006, **8**, 3433–3436; (*b*) H. Makabe, A. Kuwabara, Y. Hattori and H. Konno, A Concise Synthesis of Solamin and cis-Solamin, Mono-THF Acetogenins from Annona muricata, *Heterocycles*, 2009, **78**, 2369–2376; (*c*) H. Konno, Y. Okuno, H. Makabe, K. Nosaka, A. Onishi, Y. Abe, A. Sugimoto and K. Akaji, Total synthesis of cis-solamin A, a mono-tetrahydrofuran acetogenin isolated from Annona muricata, *Tetrahedron Lett.*, 2008, **49**, 782–785; (*d*) A. R. L. Cecil, Y. L. Hu, M. J. Vicent, R. Duncan and

 

R. C. D. Brown, Total Synthesis and Preliminary Biological Evaluation of cis-Solamin Isomers, *J. Org. Chem.*, 2004, **69**, 3368–3374; (*e*) Y. L. Hu, A. R. L. Cecil, X. Franck, C. Gleye, B. Figadère and R. C. D. Brown, Natural cis-solamin is a mixture of two tetra-epimeric diastereoisomers: biosynthetic implications for Annonaceous acetogenins, *Org. Biomol. Chem.*, 2006, **4**, 1217–1219.

24 For formal syntheses of *cis*-solamin A, see ref. 8d andK. Ota, T. Yamashita, S. Kohno, A. Miura, K. Kamaike and H. Miyaoka, Formal synthesis of cis-solamin: acid-catalyzed one-step construction of 2,5-disubstituted tetrahydrofuran, *Org. Biomol. Chem.*, 2018, **16**, 3018–3025.

25 Enantioselectivity was slightly improved (93% ee) at the lower temperature of −60 °C. The higher reaction temperature of −40 °C was beneficial in terms of rate of conversion. At 0 °C 80% ee was obtained.

26 For examples of oxidative cleavage of arylalkanols to alkanoic acids using $RuCl_3$/$NaIO_4$; M. Asaoka, M. Tanaka, T. Houkawa, T. Ueda, S. Sakami and H. Takei, Diastereodivergency in the reactions of 3-metallated-2-methylbutanamide, *Tetrahedron*, 1998, **54**, 471–486.

27 (*a*) S. Crosignani, P. D. White and B. Linclau, Microwave-accelerated O-alkylation of carboxylic acids with O-alkylisoureas, *Org. Lett.*, 2002, **4**, 2961–2963; (*b*) L. J. Mathias, Esterification and Alkylation Reactions Employing Isoureas, *Synthesis*, 1979, 561–576.

28 See SI for further details. Related tricarbonyls have been reported from permanganate oxidation of α,β-unsaturated esters; Y. Qi, Z. X. Yin, X. X. Wen, C. Wang and L. L. Zong, Permanganate oxidation of α,β-unsaturated carbonyls to vicinal tricarbonyls, *New J. Chem.*, 2023, **47**, 3249–3254.

29 (*a*) J. E. Baldwin, M. J. Crossley and E. M. M. Lehtonen, Stereospecificity of oxidative cycloaddition reactions of 1,5-dienes, *J. Chem. Soc., Chem. Commun.*, 1979, 918–920; (*b*) D. M. Walba, M. D. Wand and M. C. Wilkes, Stereochemistry of the permanganate oxidation of 1,5-dienes, *J. Am. Chem. Soc.*, 1979, **101**, 4396–4397; (*c*) S. Wolfe and C. F. Ingold, *J. Am. Chem. Soc.*, 1981, **103**, 940–941.

30 A. Poethig and T. Strassner, The Mechanism of the Permanganate-Promoted Oxidative Cyclization of 1,5-Dienes - a DFT Study, *Coll. Czech. Chem. Commun.*, 2007, **72**, 715–727.

31 For further discussion of the reoxidation of the Mn(v) glycolate intermediate, including additional DFT calculations see Computational SI..

32 (*a*) E. Záhonyi-Budó and L. I. Simándi, Oxidations with Unstable Manganese(vi) in Acidic Solution, *Inorg. Chim. Acta*, 1995, **237**, 173–175; (*b*) J. H. Sutter, K. Colquitt and J. R. Sutter, Kinetics of the disproportionation of manganate in acid solution, *Inorg. Chem.*, 1974, **13**, 1444–1446.

33 For models proposed for phase-transfer catalysed nucleophilic epoxidation of olefins see ref. 15 andB. Lygo and B. I. Andrews, Asymmetric Phase-Transfer Catalysis Utilizing Chiral Quaternary Ammonium Salts: Asymmetric Alkylation of Glycine Imines, *Acc. Chem. Res*, 2004, **37**, 518–525.

34 For computational studies on chiral phase transfer catalysis.(*a*) T. Kamachi and K. Yoshizawa, Low-Mode Conformational Search Method with Semiempirical Quantum Mechanical Calculations: Application to Enantioselective Organocatalysis, *J. Chem. Inf. Model.*, 2016, **56**, 347–353; (*b*) A. Capobianco, A. Di Mola, V. Intintoli, A. Massa, V. Capaccio, L. Roiser, M. Waser and L. Palombi, Asymmetric tandem hemiaminal-heterocyclization-aza-Mannich reaction of 2-formylbenzonitriles and amines using chiral phase transfer catalysis: an experimental and theoretical study, *RSC Adv.*, 2016, **6**, 31861–31870; (*c*) T. Kamachi and K. Yoshizawa, Enantioselective Alkylation by Binaphthyl Chiral Phase-Transfer Catalysts: A DFT-Based Conformational Analysis, *Org. Lett.*, 2014, **16**, 472–475; (*d*) G. P. Petrova, H. B. Li, K. Maruoka and K. Morokuma, Asymmetric Phase-Transfer Catalysis with Homo- and Heterochiral Quaternary Ammonium Salts: A Theoretical Study, *J. Phys. Chem. B*, 2014, **118**, 5154–5167; (*e*) T. C. Cook, M. B. Andrus and D. H. Ess, Quantum Mechanical Transition-State Analysis Reveals the Precise Origin of Stereoselectivity in Chiral Quaternary Cinchonidinium Phase-Transfer Catalyzed Enolate Allylation, *Org. Lett.*, 2012, **14**, 5836–5839; (*f*) E. J. Corey, Y. X. Bo and J. Busch-Petersen, *J. Am. Chem. Soc.*, 1998, **120**, 13000–13001.

35 The Cinchonidine-derived CPTCs **5a** and **5d** gave the same major enantiomeric products when applied to the same substrate. CPTC **5a** gave higher ee for the ketone product **19d**, whereas CPTC **5d** gave the ester THF diols **8a** and **15** with higher enantioselectivity. On this basis we selected the best performing catalyst for each substrate type.

36 F. M. Bickelhaupt and K. N. Houk, Analyzing Reaction Rates with the Distortion/Interaction-Activation Strain Model, *Angew. Chem., Int. Ed.*, 2017, **56**, 10070–10086.

37 C. Lefebvre, G. Rubez, H. Khartabil, J. C. Boisson, J. Contreras-García and E. Hénon, Accurately extracting the signature of intermolecular interactions present in the NCI plot of the reduced density gradient versus electron density, *Phys. Chem. Chem. Phys.*, 2017, **19**, 17928–17936.

38 T. Lu and Q. X. Chen, Independent gradient model based on Hirshfeld partition: A new method for visual study of interactions in chemical systems, *J. Comput. Chem.*, 2022, **43**, 539–555.